



Design and exploration of C-3 benzoic acid bioisosteres and alkyl replacements in the context of GSK3532795 (BMS-955176) that exhibit broad spectrum HIV-1 maturation inhibition

Jacob J. Swidorski^{a,*}, Susan Jenkins^{b,g}, Umesh Hanumegowda^{b,g}, Dawn D. Parker^{b,g}, Brett R. Beno^{c,f}, Tricia Protack^d, Alicia Ng^a, Anuradha Gupta^e, Yoganand Shanmugam^e, Ira B. Dicker^{d,h}, Mark Krystal^{d,g}, Nicholas A. Meanwell^{a,f}, Alicia Regueiro-Ren^{a,f}

^a Department of Discovery Chemistry, Bristol Myers Squibb Research and Development, 5 Research Parkway, Wallingford, CT 06492, USA

^b Department of Pharmaceutical Candidate Optimization, Bristol Myers Squibb Research and Development, 5 Research Parkway, Wallingford, CT 06492, USA

^c Department of Computer-Assisted Drug Design, Bristol Myers Squibb Research and Development, 5 Research Parkway, Wallingford, CT 06492, USA

^d Department of Virology, Bristol Myers Squibb Research and Development, 5 Research Parkway, Wallingford, CT 06492, USA

^e Biocon Bristol Myers Squibb Research & Development Center, Bangalore, India

ARTICLE INFO

Keywords:

HIV-1
Maturation inhibitors
Triterpene
Antiviral
GSK3532795
BMS-955176
Bioisostere

ABSTRACT

GSK3532795 (formerly BMS-955176) is a second-generation HIV-1 maturation inhibitor that has shown broad spectrum antiviral activity and preclinical PK predictive of once-daily dosing in humans. Although efficacy was confirmed in clinical trials, the observation of gastrointestinal intolerance and the emergence of drug resistant virus in a Phase 2b clinical study led to the discontinuation of GSK3532795. As part of the effort to further map the maturation inhibitor pharmacophore and provide additional structural options, the evaluation of alternates to the C-3 phenyl substituent in this chemotype was pursued. A cyclohexene carboxylic acid provided exceptional inhibition of wild-type, V370A and Δ V370 mutant viruses in addition to a suitable PK profile following oral dosing to rats. In addition, a novel spiro[3.3]hept-5-ene was designed to extend the carboxylic acid further from the triterpenoid core while reducing side chain flexibility compared to the other alkyl substituents. This modification was shown to closely emulate the C-3 benzoic acid moiety of GSK3532795 from both a potency and PK perspective, providing a non-traditional, sp³-rich bioisostere of benzene. Herein, we detail additional modifications to the C-3 position of the triterpenoid core that offer effective replacements for the benzoic acid of GSK3532795 and capture the interplay between these new C-3 elements and C-17 modifications that contribute to enhanced polymorph coverage.

HIV-1 maturation inhibitors (MIs) are a new class of therapy targeting the final step of five protease-mediated Gag protein cleavage events that occur late in the HIV-1 replication cycle.¹ Instead of binding to the protease directly, maturation inhibitors bind to the Gag protein near the junction between the capsid (CA) and spacer peptide 1 (SP1) and disturb the final and rate-limiting step of the proteolytic process. Disruption of this cleavage event interferes with the proper release of the structural proteins essential for the carefully ordered assembly of the conical core of the viral particle, resulting in virus that is unable to

complete the maturation process which ultimately compromises the iterative cycle of replication.²⁻⁴

Bevirimat (**1**) was the first HIV-1 maturation inhibitor to be advanced in clinical trials, establishing proof-of-concept for this mechanism of action (MOA).⁵ In an efficacy trial, 45% of patients administered **1** responded to therapy (designated as >0.5 log₁₀ viral load reduction) experiencing a mean viral load reduction of 1.26 log₁₀ copies/mL.⁶ However, the majority (55%) of patients experienced a minimal effect on viremia, with an average viral load reduction of 0.05

* Corresponding author at: Small Molecule Drug Discovery, Bristol Myers Squibb Research and Early Development, PO Box 4000, Princeton, NJ 08543, USA.

E-mail address: jacob.swidorski@bms.com (J.J. Swidorski).

^f Small Molecule Drug Discovery, Bristol Myers Squibb Research and Early Development, PO Box 4000, Princeton, NJ 08543, USA.

^g ViiV Healthcare, 36 East Industrial Rd., Branford, CT 06405, USA.

^h Retired from ViiV Healthcare.

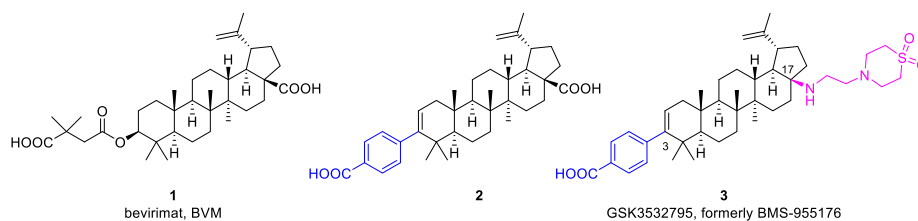


Fig. 1. Previously-disclosed HIV-1 maturation inhibitors.

\log_{10} copies/mL. Further analysis of the non-responder patient population revealed a series of distinct, naturally-occurring polymorphisms in the glutamine-valine-threonine (QVT) residues found proximal to the cleavage site at the CA-SP1 junction of the Gag polyprotein that correlated with reduced susceptibility to **1**.^{6–8}

Recent studies have identified **2** (Fig. 1), which incorporates a 4-substituted benzoic acid moiety in place of the 3'3'-dimethylsuccinate present in **1**, as an inhibitor of HIV-1 maturation that preserved the antiviral potency of **1** while significantly improving the deleterious effect of the presence of serum associated with the antiviral activity of **1**, although this compound was insufficient to address the baseline polymorphism issue.⁹ Modifications to the C-17 position of the triterpenoid core of **2** by the introduction of the (2-aminoethyl)thiomorpholine 1,1-dioxide element in **3** significantly enhanced the *in vitro* antiviral profile to encompass the most prevalent polymorphic viruses. Whereas the presence of the polymorphisms V370A and Δ V370 in the Gag protein reduced the potency of **1** compared to WT virus (55x for V370A and >1000x for Δ V370), **3** exhibited equipotent antiviral activity toward WT and V370A mutant virus while the potency shift for the Δ V370 mutant was a modest 7-fold.^{10,11} Moreover, human serum (HS) binding for **3** was 86% using an ultracentrifugation method while **1** was found to be >99% bound to HS.^{10,11} The improvements in antiviral potency and serum binding for **3** combined with a comparable preclinical PK profile to **1** supported its advancement into clinical trials.^{11,12} In the clinic, once-daily doses of 10–120 mg of **3** administered as monotherapy for 10 days were associated with a median viral load decline of 1.05–1.75 \log_{10} copies/mL in patients infected with WT HIV-1 and, importantly, similar efficacy was observed toward virus variants with pre-existing Gag polymorphisms (viral load declined by 0.97–1.98 \log_{10} copies/mL in this patient population).¹³ Unfortunately, development of **3** was suspended after completion of a phase 2b clinical trial due the observation of gastrointestinal intolerance and treatment-emergent drug resistance.¹⁴

In an effort to further understand and define the role of the C-3 substituent, additional motifs that could further enlighten the requirements at this critical element of the pharmacophore were examined in conjunction with select changes at C-17. Our efforts were focused on preserving or improving the antiviral activity inherent to **3** while differentiating the chemotype in the event of liabilities arising during development. We specifically targeted inhibition of viruses containing the key variations in the QVT region of Gag, V370A and Δ V370, in addition to maintaining inhibition of wild-type (WT) virus. The V370A-containing virus was chosen because it was the most prevalent naturally-occurring polymorphic variant in subtype B patients and exhibited 50-fold reduced susceptibility to **1** (Table 1).¹⁵ While only present in a small percentage of the subtype B patient population (0.9%), Δ V370-containing viruses showed a particularly high level of resistance (>1000 fold) to **1** and this is a common polymorphic variation in non-subtype B patients.^{10,16} Consequently, this virus was selected as a high bar sentinel for inclusion in the initial screening tier. *In vitro* potency was measured utilizing a multiple cycle replication assay in MT-2 cells using an NL4-3-derived virus expressing the Renilla luciferase gene which was incorporated as a marker for virus growth (NLRepRlucP373S). HIV-1 V370A and Δ V370 viruses were identical to the WT virus except for a single amino acid substitution (V370A) or deletion (Δ V370) at the 370 position

of the Gag protein. A Δ V370/T371A mutant virus with two amino acid substitutions was also used as a surrogate for the single mutant Δ V370 since it conferred a similar level of resistance to **3** but proved to be a more robust virus to maintain. In addition, a select subset of the compounds was evaluated against the V362I/V370A and A364V virus variants to assess the potential to inhibit viruses that are reported to confer resistance to **1**.⁸

The design of target compounds focused on further defining the spacing and geometry between the carboxylic acid extending from the C-3 position and the triterpenoid core while probing the effects of increased rigidity on the antiviral spectrum. Since the (2-aminoethyl)thiomorpholine 1,1-dioxide element at C-17 conferred optimal antiviral activity and PK properties in the context **3** and its congeners, this moiety was typically held constant although alternate C-17 elements were occasionally employed.^{17,18} It was clear from modeling studies that the C-3 modifications of **1** and **2** projected the CO₂H moiety a similar distance from the core (6.0 Å for **1** and 5.8 Å for **2**) and an energy-minimized model showed that the carboxylic acid elements extended into a topographically similar region (Fig. 2). Propionic acid **5** allowed a similar vector to be maintained but projected the CO₂H moiety a substantially shorter distance from the core (4.1 Å compared to 5.8 Å for **2**). This change corresponded with a 15-fold reduction in HIV-1 weight inhibitory potency when compared with **2**, presumably because of the shorter spacer distance. In this particular example, a CH₂OH substituent was incorporated at C-17 in place of the COOH of **1** and **2** for reasons of synthetic accessibility, a reasonable change since previous studies have shown a similar inhibition profile for compounds containing both of these variations.⁹

Conformationally mobile alkyl modifications extending from the C-3 position such as the pentanoic acid **6** maintained potent inhibition of WT HIV-1 but this compound was a 50-fold less potent inhibitor of the Δ V370/T371A variant. Although the distance from the core to the CO₂H was slightly increased compared to **3**, the added flexibility of the unsubstituted alkyl chain was detrimental to the polymorphic virus inhibition. Introduction of a *gem*-dimethyl substitution in either the 3 (**7**) or 4 (**8**) positions of the pentane side chain, designed to influence conformational mobility, fully restored potency toward Δ V370/T371A mutant in the case of **7** and partially so with **8**, reinforcing the importance of side chain topography and providing evidence that a modest increase in the distance from C-3 of the core to the carboxylic acid could be tolerated.¹⁹ In addition, within this aliphatic side chain series, **7** demonstrated the highest level of inhibition of the V362I/V370A virus that emerges in response to HIV-1 maturation inhibitors, with the EC₅₀ value reduced by almost 100-fold compared to **3**. Inhibition of A364V virus by **7** and the effects of serum on the inhibition of WT was comparable to **3**. Termination of the alkyl chain with a *bis*-carboxylic acid substituent, as in **9**, more severely affected inhibition of both WT and Δ V370/T371A viruses. Since the separation of the carboxylic acid moieties from the core appears to be reasonably close to that of the other potent compounds, the added electrostatic interactions or presumably the physicochemical properties associated with a second carboxylic acid moiety appear to be unfavorable. This was a surprising result since initial study of C-3 benzoic acid derivatives had revealed that a C-3 phenyl ring incorporating both *meta*- and *para*-carboxylic acid substituents was found to be essentially equipotent with **2**.⁹

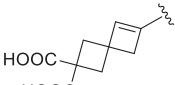
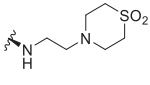

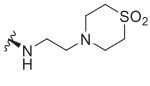
Table 1

Antiviral activity toward wild type HIV-1, V370A and Δ V370 or Δ V370/T371, V362I/V370A viruses, wild type HIV-1 with 40% human serum and 27 mg/mL human serum albumin, cytotoxicity and calculated distances between C3 and the COOH of the side chain.

C-3	C-17	<i>In vitro</i> HIV-1 inhibition EC ₅₀ (nM) ^a						CC ₅₀ (μM)	Distance C3 to COOH (Å)
		WT	V370A	Δ V370 or Δ V370/T371A ^b	V362I/V370A	A364V	WT, 40% HS + 27 mg/mL HSA-FB		
1		10	552	>10,000	–	–	–	16.8	6.0
2		16	233	>6000	–	–	316	27	5.8
3		1.9	2.7	13/23 ^b	148	1480	11.5	9.2	5.8
4		1.8	2.7	12.0	–	–	6.1	13.7	5.8
5		252	>3000	>3000	–	–	–	>10	4.1
6		2.3	–	118 ^b	–	–	–	10.2	6.5
7		1.3	–	2.3 ^b	1.6	1290	6.8	12.3	6.1
8		5.3	–	29.7 ^b	–	–	–	8.2	6.5
9		306	–	555 ^b	–	–	–	>30	5.8, 6.5
10		3.0	–	5.6 ^b	12.4	1850	–	13.5	6.9
11		2.0	–	2.2 ^b	9.7	1040	–	9.6	6.5
12		1.7	–	19.7 ^b	–	–	–	13.6	6.5
13		0.6	0.8	2.1	–	–	8.9	12.2	5.9
13a		0.9	1.3	3.1	–	–	5.7	4.1	5.9
13b		1.3	2.0	4.1	–	–	5.0	9.0	5.9
14a		2.7	–	2.7	14.7	1800	5.0	9.1	5.9
14b		1.4	–	4.2	9.6	878	6.6	13.2	5.9
15		99	39.2	40.1	113	–	–	18.6	4.9, 5.9
16		28.3 ^c	85.4	437	–	–	–	>10	6.4, 7.1
17		26.7	53.1	60.8	–	–	–	>30	5.8, 6.7

(continued on next page)

Table 1 (continued)

C-3	C-17	<i>In vitro</i> HIV-1 inhibition EC ₅₀ (nM) ^a						CC ₅₀ (μM)	Distance C3 to COOH (Å)	
		WT	V370A	ΔV370 or ΔV370/T371A ^b	V362I/V370A	A364V	WT, 40% HS + 27 mg/mL HSA-FB			
18			13	28.8	61.1	–	–	–	>30	6.4, 7.1
19			1.5	1.6	5.9	49	980	7.0	11.9	7.1

^a The antiviral activities of the compounds were assessed in a multiple cycle assay in MT-2 cells in the presence of 10% fetal bovine serum (FBS). WT, V370A, ΔV370, ΔV370/T371A EC₅₀ and CC₅₀ data are the mean of at least two experiments.

^b *In vitro* inhibition of ΔV370/T371A virus

^c All compounds were >90% pure based on ¹H NMR integration with the exception of 14. The purity of 14 was limited to 86% because poor solubility interfered with further purification attempts. ¹H NMR was used to determine purity since most of the compounds lacked a UV absorbing chromophore typically used in HPLC analysis.

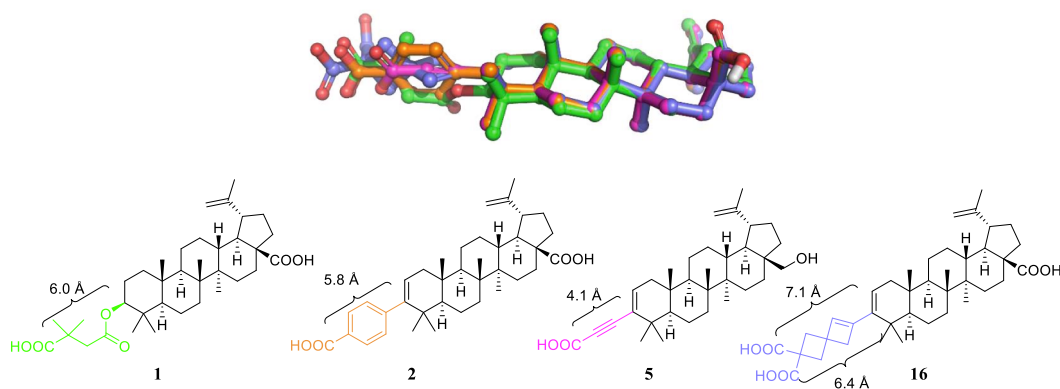


Fig. 2. Superposition of the low energy conformers of 1, 2, 5, and 16 (OPLS3/MM-GBSA). Image created with PyMOL (v 2.3 Schrödinger, LLC).

Table 2

In vivo pharmacokinetic properties of select compounds in rats^{a,†}.

#	Metabolic stability in LM, t _{1/2} (min) Human/Rat	F (%)	AUC _{0-6h} , PO (μM·h)	AUC _{total} , PO (μM·h)	t _{max} , PO (h)	C _{max} , PO (μM)	CL, IV (mL/min/kg)	V _{ss} , IV (L/kg)	C _{24h} , PO (nM)
1 ^b	>120/29.5	54 ^e	6.4 ^d	13.8 ± 1.4 ^f	1.8 ± 2 ^e	2.6 ± 0.6 ^e	5.7 ± 1 ^e	0.6 ± 0.2 ^e	6 ± 4 ^e
2 ^{b,d}	>120/>120	4	5.7 (4.7, 6.8)	–	4.0 ^g	1.3 (1.2, 1.5)	1.0 ^g	0.1 ^g	–
3 ^c	>120/>120	26	4.1 ± 0.7	14.2 ± 1.1	6.0 ± 0.0	1.2 ± 0.2	2.2 ± 0.3	1.1 ± 0.1	128 ± 27
13 ^c	58/>120	58	–	15.8 ± 5.2	2.7 ± 0.6	1.1 ± 0.5	4.3 ± 0.6	2.3 ± 0.3	196 ± 102
19 ^c	69/>120	32	–	13.5 ± 4.8	6.3 ± 1.1	0.9 ± 0.26	2.9 ± 0.5	1.4 ± 0.2	240 ± 90

[†] All studies were conducted in accordance with the GSK Policy on the Care, Welfare and Treatment of Laboratory Animals and were reviewed by the Institutional Animal Care and Use Committee either at GSK or by an ethical review process at the institution where the work was performed.

^a Each pharmacokinetic property listed is an average of the measurement from 3 rats unless otherwise noted. Doses were 5 mg/kg PO and 1 mg/kg IV.

^b Vehicle: poly(ethylene glycol) 300 (PEG 300), ethanol, Tween 80 (TW80) (89:10:1 v/v).

^c Vehicle: poly(ethylene glycol) 300 (PEG 300), ethanol, 0.1 N NaOH, Tween 80 (TW80) (84.5:10:5:0.5 v/v).

^d n = 2.

^e F(%), t_{max}, C_{max}, CL, V_{ss} and C₂₄ are reported from the full 24 h rat PK screen.

^f AUC_{total} was calculated from a full 24 h rat PK run in addition to a 6 h rat PK screen.

^g The individual value for t_{max}, CL, IV and V_{ss}, IV for 2 were within 0.1 (h, mL/min/kg and L/kg).

An element of rigidity was introduced by locking the alkyl chains through a cyclization strategy, as exemplified by analogues 10–12. Although it incorporated a longer spacer unit (6.9 Å compared to 5.8 Å for 3), the cyclohexylmethyl homolog 10, isolated as a mixture of *cis* and *trans* isomers, showed excellent antiviral properties, with WT HIV-1 inhibitory potency comparable to 3 and a ΔV370/T371A EC₅₀ of 5.6 nM. In addition, inhibition of the V362I/V370A virus was improved almost 12-fold compared to 3, although inhibitory activity toward the A364V virus was not improved. Locking the pentanoic acid moiety into a

cyclohexane ring, as in 11 and 12, maintained inhibition of WT virus in both isomers, but 11 was a several-fold more potent inhibitor of the ΔV370/T371A virus and showed equipotent inhibition of the mutant and the WT viruses. Inhibition of the V362I/V370A and the A364V viruses by 11 was similar to that of the 4-substituted analog 10. The conformation of the carboxylic acid was further constrained by attaching the ring directly to the C-3 position of the triterpenoid core via an alkene connector, as depicted by 13–19. Cyclohexene 13 is a potent inhibitor of WT, V370A and ΔV370 viruses, with a 3- to 6-fold advantage

over **3** and is subject to a similar potency shift in the presence of 10% FBS, 40% HS and 27 mg/mL HSA. In **13**, the spatial disposition of the carboxylic acid is conserved when compared to **3** and there is only a modest change in the acidity of the carboxylic acid; a cyclohexane carboxylic acid has a pK_a of 4.90 compared to a pK_a of 4.20 for benzoic acid which is lower because of conjugation of the acid moiety to the benzene ring.^{20,21} Rat PK studies with **13** showed a similar AUC_{total} (15.8 $\mu\text{M}\cdot\text{h}$), C_{max} and C_{24} with an improved oral bioavailability (F) of 58% when compared to **3** after doses of 5 mg/kg PO (Table 2). When isolated individually, both diastereoisomers **13a** and **13b** showed similar potency, although rat PK studies were not repeated with the individual isomers. The modified C-17 substituent in the ethyl-linked methylsulfonyl piperidine moiety in **14a** and **14b** was also evaluated because the corresponding benzoic acid **4** showed nearly identical in vitro potency to **3** while conferring additional structural differentiation from the clinical candidate. While WT and ΔV370 virus inhibition for **14a** and **14b** were similar to **3**, inhibition of V362I/V370A virus was improved ~10 fold while activity toward the A364V variant was comparable. Consistent with the structure-activity relationships (SARs) of the other C-3 alkyl compounds, the bis-carboxylic acid **15** was less potent.

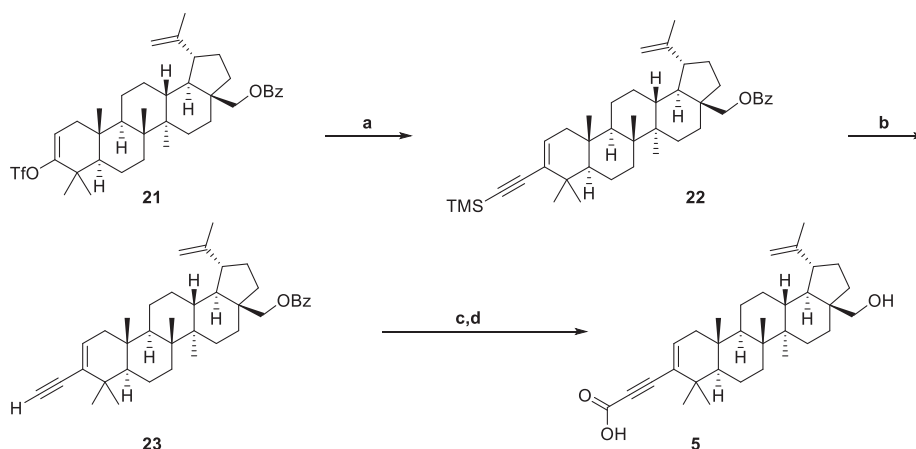
To further expand the SARs, a novel spiro[3.3]hept-5-ene was conceived as a rigid building block that could place the carboxylic acid (s) further from the triterpenoid core while retaining the geometry that appears consequential to mutant virus inhibition. In an effort to quickly probe inhibitory effectiveness of this modification, the spiro[3.3]hept-5-ene-2,2-dicarboxylic acid moiety was appended to the C-3 position in the background of a free carboxylic acid substituent at C-17, providing **16**. Intriguingly, while **16** exhibited a several-fold reduction in inhibitory potency toward WT virus compared to **1** and **2**, the only other compounds compiled in Table 1 that are not modified at C-17, inhibition of the V370A mutant virus was improved several-fold while the ΔV370 virus, which was insensitive to **1** and **2**, was inhibited with an EC_{50} of 437 nM. Molecular models of **17** indicate that one of the carboxylic acid moieties extends 6.4 Å from the core while the second carboxylic acid moiety extends further at a distance of 7.1 Å. The less distant carboxylic acid moiety projects at a downward angle, placing it adjacent to the second ring of the spirocycle rather than extending it further from the triterpenoid core.

In an effort to further improve the virological profile and the physical properties of the molecule, introduction of the (2-aminoethyl)thiomorpholine 1,1-dioxide moiety to the C-17 position was explored. Interestingly, during the synthesis of this molecule, an isomerization occurred at the diene-based junction of the C-3 spirocycle and the triterpenoid core to give a mixture of the ester precursors to **17** and **18**. The ^1H NMR chemical shift and the coupling pattern of the diene at the ring junction in **17** and **18** clearly differentiated the two isomers. Using deuterated acetic acid as the solvent, the ^1H NMR spectrum of isomer **17** was associated with two doublets with chemical shifts of 5.92 and 5.81 ppm and coupling constants of 9.8–9.9 Hz, consistent with the C-1–C-2 alkene moiety. Using the same solvent, the C-2–C-3 vinyl proton of isomer **18** resonated as a doublet of doublets with a chemical shift of 5.61 ppm and coupling constants of 6.0 and 1.6 Hz, a signal that is distinctive for compounds in this series. A singlet resonating at 5.98 ppm is consistent with the C-1'–C-2' alkene present in the spirocycle. The same alkene chemical shifts and coupling constants were observed in the ^1H NMR of the mixture of isomers that gave **20**, a closely related analog that is missing the C-17 (2-aminoethyl)thiomorpholine 1,1-dioxide moiety. In addition to the ^1H NMR data for **20**, a single crystal X-ray determination of **20** confirmed the chemical structure of this isomer. The X-ray structure showed an elongated C-1'–C-2' bond length (1.468 Å) and a shortened C-3–C-1' bond length (1.366 Å). Additionally, conjugation was apparent based on the C-1–C-2 (1.406 Å) and C-2–C-3 (1.401 Å) bond lengths. The isomerization to give **20** was observed following an alternate route which heated the spirocycle with HCl overnight; however, both **17** and **18** were sufficiently stable to be

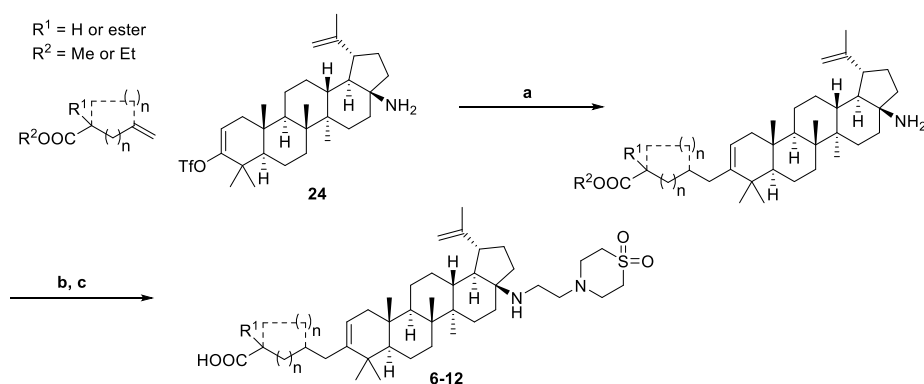
isolated by crystallization from an acidic solution at room temperature. Isomer **17** confers additional rigidification to the ring structure that constrains the placement of the two carboxylic acid moieties while isomer **18** is less rigid and allows for more movement of the carboxylic acid moieties. However, the difference in mutant virus inhibition between the two isomers was only modest. Consistent with the other series discussed above, the mono-carboxylic acid derivative of the spiro[3.3]hept-5-ene substituent provides improved inhibitory activity toward all of the viruses in the screening tier. In fact, as a mixture of diastereomers **19** displayed equivalent inhibitory potency toward the V370A and ΔV370 mutant viruses to the clinical candidate **3** even though the carboxylic acid in **19** extends 1.3 Å further from the core than in the benzoic acid-based prototype. Adding further to its potential to function as an effective bioisostere of a benzoic acid, in a rat PK study **19** exhibited similar oral exposure (AUC_{total} of 13.5 $\mu\text{M}\cdot\text{h}$, a t_{max} of 6.3 h, a C_{24} of 240 nM and F = 32%) to **3** (AUC_{total} of 14.2 $\mu\text{M}\cdot\text{h}$, a t_{max} of 6 h, a C_{24} of 128 nM and F = 26%) following doses of 5 mg/kg (Table 2).

The mode of action of betulinic acid-derived HIV-1 maturation inhibitors is beginning to emerge along with a more complete picture of the HIV-1 maturation process as the result of recent structural studies.^{23–31} X-Ray crystallography,²³ cryogenic electron tomography (Cryo-ET),^{24,25} cryogenic electron microscopy (Cryo-EM),²⁶ solid-state NMR (ssNMR)^{27–29} and computational modeling^{30,31} studies have individually and collectively provided a more detailed understanding of the mechanisms of the proteolytic processing and assembly of the hexameric capsid protein lattice. Proteolytic cleavage of the CA-SP1 peptide is a carefully choreographed process that depends upon access of HIV-1 protease to the cleavage site. The assembly of the hexameric core appears to be catalyzed by inositol hexakisphosphate (IP_6) which convenes the immature lattice bundle by engaging in electrostatic interactions with the basic residues Lys₂₉₀ and Lys₃₅₉ that are contributed by each monomer of the CA-SP1 peptide.^{32–34} In cryo-EM studies, IP_6 is located at the center of the hexameric structure between the two rings of lysine residues acting as a nidus for bundle assembly.³² How IP_6 modulates the availability of the CA-SP1 cleavage site in a conformation for proteolytic processing is not clear but in the absence of cleavage the lattice forms with the SP1 peptide still attached with the cleavage site on the inner surface of the hexameric bundle and inaccessible to the protease. After proteolytic removal of the SP1 peptide, IP_6 appears to stabilize the mature capsid protein by engaging with Arg₁₈ residues from each of the CA peptide monomers; presumably, IP_6 removal is an important element of the capsid disassembly process during infection. Thus, IP_6 promotes both the assembly, maturation and stabilization of the HIV-1 capsid while also playing a role in capsid dissolution.^{33,34} Micro electron diffraction (microED) mapping of frozen, hydrated 3D microcrystals of the CA-SP1 with and without **1** bound revealed that the maturation inhibitor binds close to the IP_6 binding site. However, while the precise orientation of **1** in the hexameric bundle was not discernible at the resolution of the experiment, modeling studies suggested that the succinic carboxylic acid moiety engaged with Lys₃₅₉ across the hexamer interface.³⁵ These observations suggest that maturation inhibitors compete with IP_6 to modulate hexamer bundle formation in a fashion that usurps the normal choreography of protease-mediated CA-SP1 cleavage. While this scenario explains the preservation of antiviral activity observed with some bis-carboxylic acid derivatives, additional insights into the SARs associated with the C-3 substituent and the precise relationship between the carboxylic acid moiety and the triterpenoid core will require the combination of higher resolution structures and a more detailed understanding of the biochemical and kinetic aspects of hexameric bundle formation and processing.

With substantial effort to develop therapeutic treatments for HIV-1 infections, patient outcomes have improved since the introduction of antiretroviral therapy. Between 1987 and 2014, more than 28 new molecular entities were developed to treat HIV/AIDS infections.³⁶ Although the pace of new discoveries in the field has slowed somewhat, new classes and combination therapies are important to treat the



Scheme 1. Preparation of C-3 alkyne **5**. Reagents and conditions: (a) TMS-acetylene, TEA, CuI, Pd(PPh₃)₄, DMF, rt, 3 h, 93%; (b) TBAF (75% in H₂O), THF, rt, 2 h, 98%; (c) *t*-BuLi, ClCO₂Et, THF, -78 °C, 2 h; (d) NaOH (1 N), 1,4-dioxane, rt, 19 h, 21% over 2 steps.

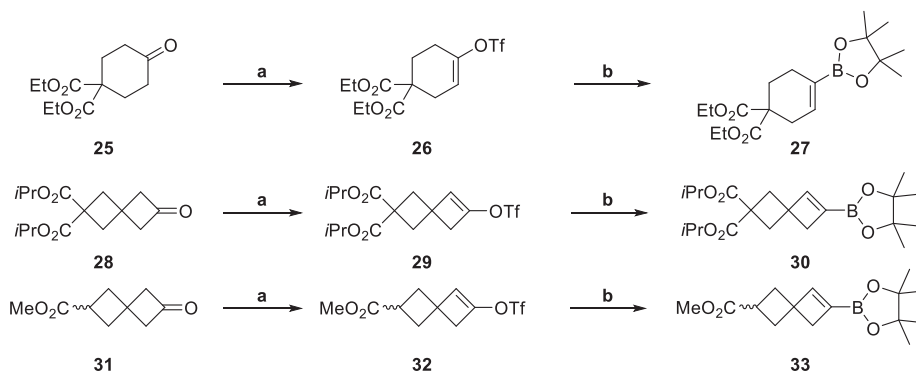


Scheme 2. β -Alkyl Suzuki-Miyaura coupling process to introduce C-3 alkyl substituents (examples **6–12**). Reagents and conditions: (a) olefin ester, 9-BBN, THF, 0 °C, rt, 2 h, then 1 M K₃PO₄, triflate, PdCl₂(dppf)-toluene adduct, 85 °C, 16–19 h; (b) 4-(2-chloroethyl)thiomorpholine 1,1-dioxide·HCl, K₃PO₄, KI, MeCN, 100 °C, 15–24 h; (c) 1 N NaOH, 1,4-dioxane, 75 °C, 3–72 h.

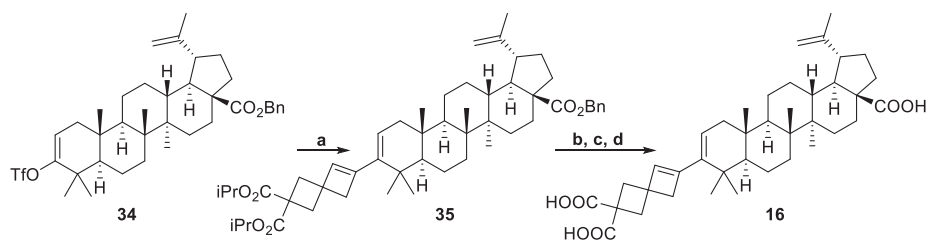
resistance that continues to emerge to existing therapies. Targeting the final step of protease-mediated Gag protein processing to inhibit the maturation of HIV-1 virions is of contemporary interest within industrial groups focused on developing mechanistically differentiated drugs and academic laboratories seeking to understand the maturation process more deeply.

The promising efficacy demonstrated by **3** in early clinical trials suggests potential for HIV-1 maturation inhibitors to be a part of future therapeutic options. However, additional structural refinement will be

required in order to surmount the gastrointestinal side effects observed with this compound after long-term dosing in the Phase 2b clinical study. The compounds described in this study offer structural differentiation at a pharmacophoric element that differs to that in **1**, which was not associated with gastrointestinal problems over long-term dosing, but further study will be required in order to understand toxicity profiles. The spiro[3.3]hept-5-ene moiety in **16–19** offers an effective, architecturally interesting and sp³-rich replacement for the phenyl ring of **3** while the cyclohexene derivatives **13–15** present a more topologically



Scheme 3. Preparation of boronate esters for C-3 Suzuki-Miyaura coupling. Reagents and conditions: (a) KHMDS (0.91 M in THF), 1,1,1-trifluoro-*N*-phenyl-*N*-((trifluoromethyl)sulfonyl)methanesulfonamide, THF, -78 °C, 5.5 h, 15–53%; (b) bis(pinacolato)diboron, KOAc, PdCl₂(dppf)-CH₂Cl₂ adduct, 1,4-dioxane, 70 °C, 5–22 h.



Scheme 4. Preparation of spiro[3.3]hept-5-ene-2,2-dicarboxylic acid **16**. Reagents and conditions: (a) **27**, bis(pinacolato)diboron, Pd(PPh₃)Cl₂, PPh₃, PhOK, toluene, 50 °C then K₃PO₄, PdCl₂(dppf)-CH₂Cl₂ adduct, DMF, 80 °C, 20%; (b) *t*-butyldimethylsilane, TEA, Pd(OAc)₂, DCE, 60 °C; (c) aq. TBAF, THF, rt; (d) NaOH, 1,4-dioxane, 75 °C, 44% over 3 steps.

faithful phenyl bioisostere that offers the potential for the introduction of substituents that explore topographical space not available by substitution of the 2-dimensional phenyl ring of **3**.

The synthesis of alkyne **5** employed a Sonigashira coupling of triflate intermediate **21**⁹ with TMS-acetylene as the coupling partner to give **22** (Scheme 1). The TMS-protected intermediate **22** was unmasked by treating with aqueous tetrabutylammonium fluoride (TBAF) solution in THF at room temperature to give **23** which was deprotonated with *t*-BuLi and the acetylide treated with ethyl chloroformate to give the alkynyl ester. Both the alkynyl carboxylic acid and the C-28 alcohol were deprotected using aqueous NaOH to provide **5**.

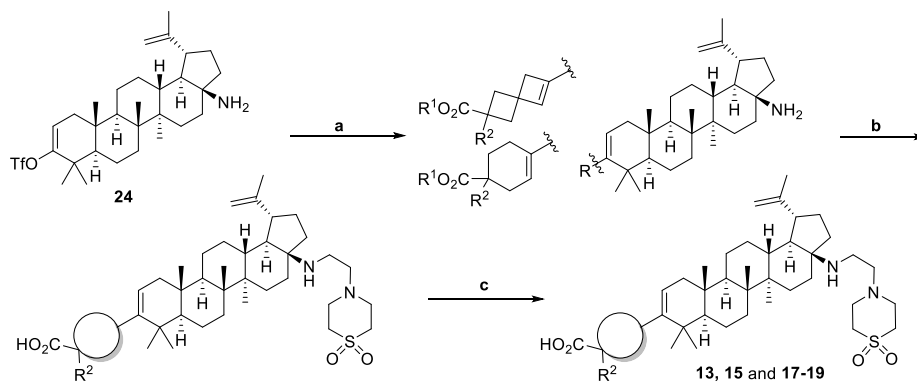
Installation of alkyl substituents at the C-3 position was achieved using β -alkyl Suzuki-Miyaura conditions (Scheme 2).³⁷ Terminal olefins with pendent alkyl esters were converted to alkyl boranes via hydroboration using 9-BBN followed by palladium-catalyzed cross-coupling with the vinyl triflate **24** to give the C-3 alkylated products. Alkylation of the C-17 amine utilizing 4-(2-chloroethyl) thiomorpholine 1,1-dioxide,¹² K₃PO₄ and KI in acetonitrile heated to 100 °C in a sealed tube followed. The ester of the C-3 alkyl chain was hydrolyzed with aqueous NaOH to give carboxylic acids **6–12**.

The preparation of the C-3 modified analogs **13–19** employed a strategy utilizing Suzuki-Miyaura coupling of a boronate ester with the vinyl triflate intermediates **24** and **34**. Boronate ester **27** was prepared by a process that began with deprotonation of ketone **25** with potassium bis(trimethylsilyl)amide (KHMDS) at –78 °C followed by treatment with 1,1,1-trifluoro-*N*-phenyl-*N*-((trifluoromethyl)sulfonyl)methanesulfonamide to give the vinyl triflate **25** (Scheme 3). Conversion of the vinyl triflate **26** to the boronate ester **27** was accomplished using bis(pinacolato)diboron, KOAc and PdCl₂(dppf)-CH₂Cl₂ adduct while heating to 70 °C in 1,4-dioxane. Preparation of the di-carboxylate analog **30** and the mono-carboxylate boronate ester **33** were accomplished using the same two step sequence from ketones **28** and **31**.³⁸ It should be noted that both **27** and **33** were used in the subsequent Suzuki-Miyaura coupling steps with impurities present that were difficult to remove

because of the very non-polar nature of the compounds. Although the yield for the initial formation of the vinyl triflate was quite variable from one ketone to the next, sufficient material was prepared using this methodology to deliver these analogs.

After difficulty using standard Pd(PPh₃)₄ conditions for the Suzuki-Miyaura coupling of vinyl triflate **34** to boronate ester **30**, the reverse process in which a C-3 vinyl boronate ester (not shown) was coupled with the vinyl triflate intermediate **29** was attempted but without success. Consequently, a modification of the conditions developed by Miyaura and co-workers was employed to accomplish the coupling (Scheme 4).³⁹ In a one-pot sequence, vinyl triflate **29** was converted to the boronate ester to which the vinyl triflate **34** was added along with a secondary catalyst and base to achieve the coupling and provide the C-3 spiro[3.3]hept-5-ene-2,2-dicarboxylic ester **35**.⁹ Intermediate **35** was carried into the next series of reactions in the presence of some chromatographically close impurities in anticipation that they would more easily be removed after subsequent steps. A three-step sequence to deprotect the carboxylic acids on both the spirocycle and the C-17 carboxylic acid was then used to give **16**. The C-17 benzyl group was converted to a TBDMS-protected carboxylic acid using Pd(OAc)₂, TEA and *t*-butyldimethylsilane. The TBDMS group was removed using aqueous TBAF and the remaining carboxylic acids unmasked via hydrolysis of the carboxylic esters using NaOH to give **16**. Although the compound still had sub-optimal purity (86%) after the first purification by preparative HPLC, further purification was complicated because of the poor solubility in typical preparative HPLC or crystallization solvents. This compound was tested in the antiviral assays in impure form in order to obtain a measure of the potency and thus the potential of the chemotype.

The preparation of compounds **13**, **15** and **17–19** were accomplished in a straightforward manner using the Suzuki-Miyaura coupling of vinyl triflate **24**⁹ with the corresponding boronate esters (Scheme 5). After the Suzuki-Miyaura coupling, alkylation of the C-17 amine was accomplished utilizing 4-(2-chloroethyl) thiomorpholine 1,1-dioxide·HCl,



Scheme 5. Preparation of cycloalkene analogs **13**, **15** and **17–19**. Reagents and conditions: (a) Boronate ester, Pd(PPh₃)₄, Na₂CO₃·H₂O, 1,4-dioxane, H₂O, 85 °C, 5–21 h or boronate ester, S-phos, Pd(OAc)₂, K₃PO₄, 1,4-dioxane, H₂O, 75 °C; (b) 4-(2-chloroethyl)thiomorpholine 1,1-dioxide·HCl, K₃PO₄, KI, MeCN, 100–120 °C, 15–22 h; (c) aq. NaOH, 1,4-dioxane, 65–85 °C, 15–83 h.

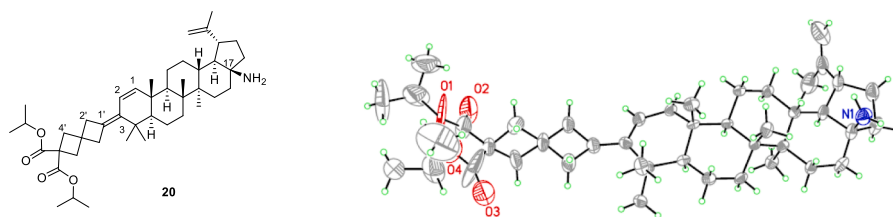
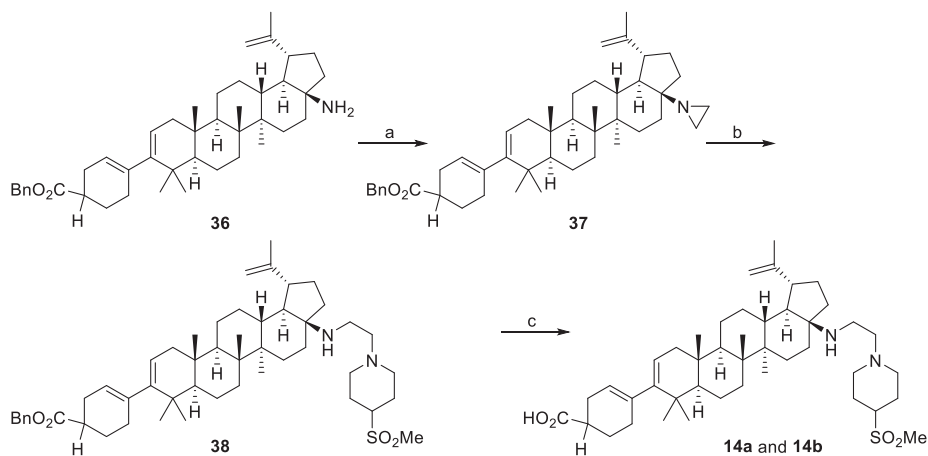


Fig. 3. ORTEP depiction of the single crystal X-ray structure of **20**.²²



Scheme 6. Preparation of cycloalkene analogs **14a** and **14b**. Reagents and conditions: (a) $\text{BrCH}_2\text{CH}_2\text{Cl}$, K_3PO_4 , MeCN, 120 °C, 23–24 h; (b) 4-(methylsulfonyl)piperidine, 1,4-dioxane, DIPEA, 1,4-dioxane, 95–100 °C, 15–23 h; (c) NaOH (1 N), 1,4-dioxane, 60 °C, 4–5 h.

K_3PO_4 , KI in acetonitrile heated to 100–120 °C in a sealed tube. The alkylated intermediates were treated with aq. NaOH to hydrolyze the carboxylate appendages of the cycles introduced from the Suzuki-Miyaura coupling step to the carboxylic acids. Interestingly, two isomers were formed during the alkylation step en route to **18**. The two isomers were separated by supercritical fluid chromatography (SFC) after the final hydrolysis to give **17** and **18**. Structural identification of isomer **17** was confirmed by comparison of the spectroscopic data to the data from the C-17 amine intermediate **20** (Fig. 3) formed from a different synthetic route that encountered difficulties, but allowed for the determination of a single crystal X-ray structure which confirmed the assignment.

The preparation of compounds **14a** and **14b** employed alternate Suzuki-Miyaura coupling conditions utilizing S-phos ligand and Pd (OAc)₂ to combine the chiral boronate esters⁴⁰ with the vinyl triflate **24** (Scheme 5). The C-17 amine **36** was alkylated with 1-bromo-2-chloroethane using K_3PO_4 in CH_3CN at 120 °C in a sealed tube to provide the aziridine **37** which was subsequently opened with 4-(methylsulfonyl)piperidine to give the ethyl-linked methylsulfonyl piperidine **38**. The cyclohexene esters were hydrolyzed to the corresponding carboxylic acids **14a** and **14b** using aqueous NaOH (Scheme 6).

Declaration of Competing Interest

The authors declare that they have no known competing financial interests or personal relationships that could have appeared to influence the work reported in this paper.

Acknowledgement

The authors gratefully acknowledge the bioanalytical group, Qi Gao and Amy Sarjeant for their X-ray crystallography support and Stella Huang for her provision of spectroscopic data. In addition, we would like to recognize Nanjundaswamy Kanikahalli Chikkananjunda, Duraisamy

Ramasamy, Richard Rampulla, Arvind Mathur and the Bristol Myers Squibb Department of Discovery Synthesis for providing key intermediates which were used to synthesize several of the compounds described in this manuscript.

Appendix A. Supplementary data

Supplementary data to this article can be found online at <https://doi.org/10.1016/j.bmcl.2021.127823>.

References

- (a) Lingappa JR, Reed JC, Tanaka M, Chutiraka K, Robinson BA. *Virus Res.* 2014; 193:89–107. <https://doi.org/10.1016/j.virusres.2014.07.001>. (b) Bell, Neil M, Lever AML. *Trends Microbiol.* 2013;21:136–144. <https://doi.org/10.1016/j.tim.2012.11.006>. (c) Lee SK, Potempa M, Swanstrom R. *J Biol Chem.* 2012;287. <https://doi.org/10.1074/jbc.R112.399444>, 867–840,874.
- Sundquist WI, Kräusslich HG. *Cold Spring Harb Perspect Med.* 2012;7, a006924. <https://doi.org/10.1101/cshperspect.a006924>.
- Li F, Goila-Gaur R, Salzwedel K, et al. *Proc Natl Acad Sci USA.* 2003;100: 1355–13560. <https://doi.org/10.1073/pnas.2234683100>.
- Zhou J, Yuan X, Dismuke D, et al. *J Virol.* 2004;78:922–929. <https://doi.org/10.1128/JVI.78.2.922-929.2004>.
- (a) Smith PF, Ogundele A, Forrest JW, et al. *Antimicrob Agents Chemother.* 2007;51: 3574–3581. <https://doi.org/10.1128/AAC.00152-07>. (b) Martin DE, Blum R, Wilton J, et al. *Antimicrob Agents Chemother.* 2007;51:3063–3066. <https://doi.org/10.1128/AAC.01391-06>.
- McCallister S, Lalezari J, Richmond G, et al. *Antiviral Ther.* 2008;13:A10.
- Van Baelen KV, Salzwedel K, Rondelez E, et al. *Antimicrob Agents Chemother.* 2009;53: 2185–2188. <https://doi.org/10.1128/AAC.01391-06.10.1128/AAC.01650-08>.
- (a) Margot NA, Gibbs CS, Miller MD. *Antimicrob Agents Chemother.* 2010;54: 2345–2353. <https://doi.org/10.1128/AAC.01784-09>. (b) Knapp DJHF, Harrigan RP, Poon AFY, Brumme ZL, Brockman M, Cheung PK. *J Clin Microbiol.* 2011;49:201–208. <https://doi.org/10.1128/JCM.01868-10>. (c) Dicker I, Zhang S, Ray N, et al. *PLoS One.* 2019;14, e0224076. <https://doi.org/10.1371/journal.pone.0224076>.
- Liu Z, Swidorski JJ, Nowicka-Sans B, et al. *Bioorg Med Chem.* 2016;24:1757–1770. <https://doi.org/10.1016/j.bmc.2016.03.001>.
- Nowicka-Sans B, Protack T, Lin Z, et al. *Antimicrob Agents Chemother.* 2016;60: 3956–3969. <https://doi.org/10.1128/AAC.02560-15>.
- Regueiro-Ren A, Liu Z, Chen Y, et al. *ACS Med Chem Lett.* 2016;7:568–572. <https://doi.org/10.1021/acsmchemlett.6b00010>.

- 12 Regueiro-Ren A, Swidorski JJ, Liu Z, et al. *J Med Chem*. 2018;61:7289–7313. <https://doi.org/10.1021/acs.jmedchem.8b00854>.
- 13 Hwang C, Schurmann D, Sobotha C, et al. *Clin Infect Dis*. 2017;65:442–452. <https://doi.org/10.1093/cid/cix239>.
- 14 Morales-Ramirez J, Bogner JR, Molina J-M, et al. *PLoS One*. 2018;13. <https://doi.org/10.1371/journal.pone.0205368>.
- 15 (a) Lu W, Salzwedel K, Wang D, et al. *Antimicrob Agents Chemother*. 2011;55:3324. (b) Seclén E, González M, Corral A, Mendoza C, Soriano V, Poveda E. *AIDS*. 2010;24:467–469. <https://doi.org/10.1097/QAD.0b013e3283335ce07>.
- 16 Dang Z, Ho P, Zhu L, et al. *J Med Chem*. 2013;56:2029–2037. <https://doi.org/10.1021/jm3016969>.
- 17 Swidorski JJ, Liu Z, Sit S-Y, et al. *Bioorg Med Chem Lett*. 2016;26:1925–1930. <https://doi.org/10.1016/j.bmcl.2016.03.019>.
- 18 Chen Y, Sit S-Y, Chen J, et al. *Bioorg Med Chem Lett*. 2018;28:1550–1557. <https://doi.org/10.1016/j.bmcl.2018.03.067>.
- 19 Jung ME, Piizzi G. *Chem Rev*. 2005;105:1735–1766. <https://doi.org/10.1021/cr940337h>.
- 20 University of Wisconsin pKa Data Compilation by R. Williams. https://www.chem.wisc.edu/areas/reich/pkatable/pKa_compilation-1-Williams.pdf [Accessed online May 08, 2020].
- 21 Gunaydin H, Bartberger MD. *ACS Med Chem Lett*. 2016;7:341–344. <https://doi.org/10.1021/acsmedchemlett.6b00099>.
- 22 The X-ray crystal structure coordinates have been deposited in the or Cambridge Crystallographic Data Centre as CCDC 2031147.
- 23 Wagner JM, Zadrozny KK, Chrustowicz J, et al. *eLife*. 2016. <https://doi.org/10.7554/eLife.17063>.
- 24 Schur FKM, Obr M, Hagen WJH, et al. *Science*. 2016;353:506–508. <https://doi.org/10.1126/science.aaf9620>.
- 25 Schur FKM, Hagen WJH, Rumlová M, et al. *Nature*. 2015;517:505–508. <https://doi.org/10.1038/nature13838>.
- 26 Bharat TAM, Menendez LRC, Hagen WJH, et al. *Proc Natl Acad Sci USA*. 2014;111:8233–8238. <https://doi.org/10.1073/pnas.1401455111>.
- 27 Han Y, Hou G, Suiter CL, et al. *J Am Chem Soc*. 2013;135. <https://doi.org/10.1021/ja406907h>, 793–717,803.
- 28 Bayro MJ, Ganser-Pornillos BK, Zadrozny KK, Yeager M, Tycko R. *J Am Chem Soc*. 2016;138:12029–12032. <https://doi.org/10.1021/jacs.6b07259>.
- 29 Gupta S, Louis JM, Tycko R. *Proc Natl Acad Sci USA*. 2020;117:10286–10293. <https://doi.org/10.1073/pnas.1917755117>.
- 30 Goh BC, Perilla JR, England MR, Heyrana KJ, Craven RC, Schulten K. *Structures*. 2015;23:1414–1425. <https://doi.org/10.1016/j.str.2015.05.017>.
- 31 Tomasini MD, Johnson DS, Mincer JS, Simon SM. *PLoS One*. 2018;13, e0196133. <https://doi.org/10.1371/journal.pone.0196133>.
- 32 Dick RA, Zadrozny KK, Xu C, et al. *Nature*. 2018;560:509–512.
- 33 Mallery DL, Márquez CL, McEwan WA, Dickson CF, et al. *eLife*. 2018. <https://doi.org/10.7554/eLife.35335>.
- 34 (a) Obr M, Kräusslich H-G. *eLife*. 2018. <https://doi.org/10.7554/eLife.38895>. (b) Kleinpeter AB, Freed EO. *Viruses*. 2020;12:940. <https://doi.org/10.3390/v12090940>.
- 35 Purdy MD, Shi D, Chrustowicz J, Hattne J, Gonen T, Yeager M. *Proc Natl Acad Sci USA*. 2018;115:13258–13263. <https://doi.org/10.1073/pnas.1806806115>.
- 36 Kinch MS, Patridge E. *Drug Discov Today*. 2014;19:1510–1513. <https://doi.org/10.1016/j.drudis.2014.05.012>.
- 37 Miyaura N, Ishiyama T, Sasaki H, Ishikawa M, Sato M, Suzuki A. *J Am Chem Soc*. 1989;111:314–321. <https://doi.org/10.1021/ja00183a048>.
- 38 Radchenko DS, Grygorenko OO, Komarov IV. *Tetrahedron Asymmetry*. 2008;19:2924–2930.
- 39 Takagi J, Takahashi K, Ishiyama T, Miyaura N. *J Am Chem Soc*. 2002;124:8001–8006. <https://doi.org/10.1021/ja0202255>.
- 40 Swidorski J, Meanwell NA, Regueiro-Ren A, Sit S-Y, Chen J, Chen, Y. US 8,906,889 B2. Dec. 09, 2014.